NeuroImage: Clinical 22 (2019) 101692

Contents lists available at ScienceDirect

NeuroImage: Clinical

journal homepage: www.elsevier.com/locate/ynicl

Reduced higher dimensional temporal dynamism in neurofibromatosis type 1

Eva Mennigen[a], Peter Schuette[a], Ariana Vajdi[a], Laura Pacheco[a], Tena Rosser[c,d], Carrie E. Bearden[a,b,*]

[a] Department of Psychiatry and Biobehavioral Sciences, University of California, Los Angeles, CA, USA
[b] Department of Psychology, University of California, Los Angeles, CA, USA
[c] Children's Hospital Los Angeles, Los Angeles, CA, USA
[d] University of Southern California, Keck School of Medicine, Los Angeles, CA, USA

ARTICLE INFO

Keywords:
Neurofibromatosis type 1
Functional connectivity
Dynamic functional network connectivity
Meta-state analysis
Group independent component analysis

ABSTRACT

Neurofibromatosis type 1 (NF1) is a common single gene disorder resulting in multi-organ involvement. In addition to physical manifestations such as characteristic pigmentary changes, nerve sheath tumors, and skeletal abnormalities, NF1 is also associated with increased rates of learning disabilities, attention deficit hyperactivity disorder, and autism spectrum disorder. While there are established NF1-related structural brain anomalies, including brain overgrowth and white matter disruptions, little is known regarding patterns of functional connectivity in NF1. Here, we sought to investigate functional network connectivity (FNC) in a well-characterized sample of NF1 participants (n = 30) vs. age- and sex-matched healthy controls (n = 30). We conducted a comprehensive investigation of both static as well as dynamic FNC and meta-state analysis, a novel approach to examine higher-dimensional temporal dynamism of whole-brain connectivity.

We found that static FNC of the cognitive control domain is altered in NF1 participants. Specifically, connectivity between anterior cognitive control areas and the cerebellum is decreased, whereas connectivity within the cognitive control domain is increased in NF1 participants relative to healthy controls. These alterations are independent of IQ.

Dynamic FNC analysis revealed that NF1 participants spent more time in a state characterized by whole-brain hypoconnectivity relative to healthy controls. However, connectivity strength of dynamic states did not differ between NF1 participants and healthy controls.

NF1 participants exhibited also reduced higher-dimensional dynamism of whole-brain connectivity, suggesting that temporal fluctuations of FNC are reduced. Given that similar findings have been observed in individuals with schizophrenia, higher occurrence of hypoconnected dynamic states and reduced temporal dynamism may be more general indicators of global brain dysfunction and not specific to either disorder.

1. Introduction

Neurofibromatosis type 1 (NF1) is an autosomal dominant genetic disorder caused by a mutation in the neurofibromin gene on chromosome 17q11.2. This tumor suppressor gene mediates cellular signaling pathways controlling cell growth (Gutmann et al.,1991), and thus mutations in this gene lead to growth of the eponymous neurofibromas, benign tumors deriving from the nerve sheaths of peripheral and spinal nerves. However, individuals with NF1 also have an increased risk of developing malignancies, and life expectancy is reduced (see (Gutmann et al., 2017) for an excellent primer on NF1). In addition to neurofibromas, other diagnostic criteria include café-au-lait macules, axillary or groin freckling, optic pathway gliomas, iris hamartomas, bone dysplasia, and having a first degree relative with NF1. Clinical presentation varies widely between individuals, and the disorder progresses throughout the life span.

In addition to these diverse symptoms that affect multiple organ systems, NF1 is also associated with increased rates of learning disabilities, attention deficit hyperactivity disorder (ADHD, (Hyman et al., 2005; Lidzba et al., 2012)), and autism spectrum disorder (ASD, (Chisholm et al., 2018; Garg et al., 2013)). Because of its single gene etiology, NF1 is a valuable model to study neural underpinnings of these neurodevelopmental disorders by means of functional and structural magnetic resonance imaging (MRI). Overall, gray and white

* Corresponding author at: UCLA Semel Institute for Neuroscience & Human Behavior, 760 Westwood Plaza, Los Angeles, CA 90095, USA.
E-mail address: cbearden@mednet.ucla.edu (C.E. Bearden).

https://doi.org/10.1016/j.nicl.2019.101692
Received 10 September 2018; Received in revised form 11 January 2019; Accepted 27 January 2019
Available online 29 January 2019

matter volumes are increased in NF1 participants; applying diffusion tensor imaging to study white matter microstructural changes in NF1 individuals, it has been shown that integrity of white matter fiber tracts is disrupted, most prominently in the frontal lobe (Karlsgodt et al., 2012). While structural connectivity can be viewed as the physical backbone of functional connectivity, these modalities yield complementary information (Damoiseaux and Greicius, 2009; Honey et al., 2009; Skudlarski et al., 2008; van den Heuvel et al., 2009).

With regard to functional connectivity in NF1, most commonly assessed during resting-state functional MRI (rs-fMRI), few studies have been published to date. A pharmacologic intervention study in 7 children with NF1 tested the effects of lovastatin, an inhibitor of the Ras signaling pathway (Costa et al., 2002), on functional connectivity within the default mode network (DMN) (Chabernaud et al., 2012). Long-range anterior-posterior connectivity of the DMN increased and therefore appeared to 'normalize' under treatment with lovastatin, although the absence of a control group makes interpretation of these findings difficult. Applying a novel graph theoretic approach, Tomson et al. replicated these findings of reduced long-range anterior-posterior connectivity in adolescent and adult participants with NF1 relative to healthy controls (Tomson et al., 2015). Specifically, this study found that the anterior brain regions identified in their study belonged to the cognitive control domain, a functional network facilitating higher executive functions such as response inhibition, performance monitoring, and working memory (Luna et al., 2015).

Given recent evidence that functional connectivity is not static over the course of a typical rs-fMRI scan (Allen et al., 2012a; Hutchison et al., 2013b; Matsui et al., 2018), we sought to complement these traditional methods by capturing patterns of dynamic functional network connectivity (FNC) to characterize variation across the resting scan (Calhoun et al., 2001; Calhoun and Adali, 2012; Erhardt et al., 2011), utilizing the same sample as in Tomson et al. Additionally, in order to yield a comprehensive overview of resting FNC in NF1 we conducted a meta-state analysis (Miller et al., 2016), a novel method to investigate temporal fluctuations of whole-brain connectivity, thereby yielding information about the dynamic fluidity and range of whole-brain connectivity in each individual. Whereas dynamic FNC follows a 'hard-clustering' approach, where connectivity captured in time windows is assigned to the one dynamic state it shows highest similarity with, the meta-state approach allows for dynamic states to overlap in time by creating a higher-dimensional state space. Further, we conducted post hoc analyses to investigate whether observed functional connectivity patterns were mediated by IQ or ADHD diagnosis.

2. Material & methods

2.1. Participants

Thirty individuals diagnosed with NF1 were recruited for this study from the greater Los Angeles area, via Institutional Review Board (IRB)-approved advertisements at the University of California, Los Angeles (UCLA) and other local medical centers. Data from 30 age- and sex-matched individuals were gathered from a pool of healthy study participants (Poldrack et al., 2016). All study participants provided informed written consent after study procedures were fully explained, according to approval from the IRB at UCLA. All participants were determined to meet criteria for NF1 based on the diagnostic criteria specified by the National Institutes of Health Consensus Development Conference through a physical examination and a clinical interview by a physician familiar with the disorder (TR).

The Structured Clinical Interview for DSM IV (First et al., 2002) was administered to healthy control participants in order to rule out any major mental illness. General exclusion criteria encompassed significant substance use in the last 6 months, a history of head injury, IQ < 70, and insufficient fluency in English. Demographic information of the sample is provided in Table 1.

Table 1
Demographics.

	Healthy controls	NF 1	p-value
Age (mean, SD, range)	25.5 (11.1); 10–45	27.1 (12.1); 10–46	0.6
Sex, N (% female)	14 (47)	18 (60)	0.3
Full Scale IQ, mean (SD)	113 (19.1)	97 (12.6)	< 0.001
ADHD flag, N (%)	4[+] (13.3)	11 (36.7)	0.06
Motion, mean, in mm (SD)	0.27 (0.21)	0.16 (0.31)	0.19

NF1 – neurofibromatosis type 1; SD – standard deviation; ADHD – attention deficit hyperactivity disorder.
[+] Data not available for 3 participants.

2.2. Clinical assessment

The Wechsler Abbreviated Scale of Intelligence was administered to all participants to estimate Full-Scale IQ (Wechsler, 1999). In order to assess ADHD symptomatology, the Child Behavioral Checklist (CBCL, (Achenbach, 1991)) was administered to participants younger than 18 years whereas older participants completed the Adult ADHD Self-Report Scale (ASRS, (Kessler et al., 2005)). For the CBCL, we applied a suggested cut-off score of 60 ('borderline') on the Attention Problems Scale (Roessner et al., 2007) to identify individuals with probable ADHD. For the ASRS, the cut-off was 4 points, i.e. one point for items 1–3 if the item score is ≥ 2 and one point for items 4–6 if the item score is ≥ 3 (Adler et al., 2006; Kessler et al., 2007, 2005). In total, 11 individuals with NF1 were flagged as having probable ADHD vs. 4 healthy participants (Table 1).

2.3. Magnetic resonance imaging data acquisition

Protocols for the rs-fMRI scans were identical for all participants, and all scans were acquired with identical 3T Siemens Tim Trio magnets with identical software. Eyes-open resting state scans were acquired over 5 min (152 volumes, voxel size 3 × 3 × 4 mm, repetition time (TR) = 2 s, echo time (TE) = 30 ms, flip angle 90 degrees, field-of-view (FOV) 192mm^2, matrix size 64 × 64). Individuals were either scanned at the Ahmanson-Lovelace Brain Mapping Center or at the Staglin Center for Cognitive Neuroscience both located at UCLA (see Supplementary Material for details); effects of scanner site were regressed out prior to statistical analyses.

A T1-weighted MPRAGE high-resolution structural scan was collected from each participant which was used to co-register functional scans during the pre-processing step (sequence details: voxel size 1 × 1 × 1.2 mm, TR = 2.3 s, TE = 2.89 ms, flip angle 9 degrees, FOV 256 mm^2).

Structural images were inspected for structural abnormalities prior to the analysis of resting state scans by a clinician experienced with NF1 (TR). To further investigate gray matter morphology differences between the two groups, we performed a Freesurfer (http://surfer.nmr.mgh.harvard.edu/) analysis of surface area, cortical thickness, and volume (see Supplementary material).

2.4. Resting state fMRI pre-processing

A combination of FMRIB Software Library (FSL; https://fsl.fmrib.ox.ac.uk/fsl) and Analysis of Functional NeuroImages (AFNI; https://afni.nimh.nih.gov) tools were utilized for the preprocessing of rs-fMRI data. The first four volumes were discarded in order to allow for equilibration effects. Slice time correction was applied in order to correct for acquisition offset between slices. Images were reoriented and FSL Motion Correction Linear Image Registration Tool (MCFLIRT, (Jenkinson et al., 2002)) was used for motion correction and co-registration into MNI standard space. Skull stripping was performed and images were spatially smoothed with a 5 mm full-width at half-maximum (FWHM) kernel.

Analysis of the association between age and mean frame-wise displacement can be found in the supplementary material.

3. Functional network connectivity analysis

3.1. Group Independent Component Analysis (ICA)

We used the Group ICA fMRI toolbox (GIFT, http://mialab.mrn.org/software/gift) to perform spatial group independent component analysis (ICA) with a high model order of $n = 100$ (Calhoun et al., 2001; Calhoun and Adali, 2012). Spatial group ICA decomposes the rs-fMRI data into spatially independent components. First, two data reduction steps are implemented, applying principal component analysis (PCA): (1) for each subject the number of time points was reduced from 148 to 120 principal components, and (2) subject-wise reduced data were concatenated across the entire group and were further reduced to 100 principal components applying the expectation-maximization algorithm (Roweis, 1998) as implemented in GIFT. Then, infomax ICA was repeated 10 times in ICASSO (Himberg and Hyvärinen, 2003), a software package designed to investigate reliability of ICA runs, in order to ensure stability of estimation. ICA yielded 100 independent components consisting of a spatial map with a corresponding time course. Subject-specific spatial maps and time courses were derived using spatial-temporal back-reconstruction (Erhardt et al., 2011). All analysis steps are shown in Fig. 1a.

These 100 independent components were evaluated to identify "meaningful" intrinsic connectivity networks (ICNs), i.e., independent components that represent anatomical brain regions. These meaningful ICNs show peak activation in gray matter with minimal overlap with white matter, ventricles, blood vessels, and non-brain structures, and their power spectra show highest power in the lowest frequencies (Allen et al., 2012b, 2011). Out of 100 components, 41 were identified as ICNs and were categorized into 9 functional domains based on their anatomic location and scientific literature using the automated anatomic labeling atlas (AAL; Tzourio-Mazoyer et al., 2002) and neurosynth.org: subcortical (SC), salience (SAL), auditory (AUD), sensorimotor (SM), visual (VIS), cognitive control (CC), default mode network (DMN), limbic, and cerebellar (CB), see Fig. 2.

3.2. Postprocessing of time courses

Postprocessing of time courses was performed as implemented in GIFT and included linear, quadratic, and cubic detrending and regression of 6 motion parameters (x-, y-, z-direction, pitch, roll, and yaw) plus their derivatives and squares (Power et al., 2014) in order to reduce motion-related artifacts. Further, time courses were despiked (spike = root mean square of the frame-wise displacement > 0.5 mm) using AFNI's 3Ddespike and interpolated using a 3rd order spline fit to clean neighboring data. A 5th order Butterworth filter was used for temporal filtering (passband 0.001–0.15 Hz).

3.3. Static Functional Network Connectivity (FNC)

Based on the processed time courses, FNC can be calculated as Pearson's correlation between all ICNs, yielding one single FNC matrix that averages connectivity across the resting state scan, i.e., static FNC. In the first analysis, we tested for group differences in static FNC. We used the MANCOVAN toolbox (Allen et al., 2011) implemented in GIFT, testing for effects of group (NF1 vs. HC), age, and sex while controlling for scanner site as a nuisance variable and regressing out motion parameters. We performed two types of analysis: one including all ICN-to-ICN connections (41×41 matrix) and one in which connectivity was averaged across domains (9×9 matrix). Results were corrected for multiple comparisons applying false discovery rate (FDR) correction ($q = 0.05$).

Since IQ and the proportion of probable ADHD differed between groups, we tested post hoc whether significant FNC results were mediated by IQ and/or ADHD utilizing the *mediation* package in R (https://cran.r-project.org/web/packages/mediation/vignettes/mediation.pdf). As suggested in the approach by Imai et al. (Imai et al., 2011, 2010a, 2010b), first two separate regression models are estimated: One model for the association between the mediator and the independent variable, i.e., group, plus a set of covariates (age and sex), and one for the association between the dependent variable, i.e., FNC, and the mediator, independent variable, and the set of covariates. Given that IQ was significantly lower in NF1 participants, we modeled the interaction of group by IQ. Based on the model fits from both models, the average causal mediation effect (ACME) and the average direct effect (ADE, i.e., the effect of the independent variable on the dependent variable, corrected for potential mediation effects and the effect of covariates) can be estimated (Imai et al., 2011, 2010a, 2010b). Bootstrapping with 1000 simulations was applied in order to ensure stability of estimations.

3.4. Dynamic functional network connectivity

Recent studies have shown that FNC has dynamic properties (Matsui et al., 2018). With regard to rs-fMRI data, dynamic behavior of FNC can be captured, for example, by applying a sliding window approach (Allen et al., 2012a). In this approach, FNC is first estimated within smaller portions of the time course (tapered windows with a size of 30 TRs = 60s). Then, these windowed FNC matrices are used to identify recurring patterns of whole-brain connectivity via *k*-means clustering, yielding distinct 'states' (see Fig. 1 for further details). The optimal number of clusters can be estimated based on objective criteria like the elbow criterion that reflects the ratio of within- to between-cluster distances while testing for different numbers of *k*. The elbow criterion suggested $k = 3$ clusters in the current study.

We used Matlab's (Release 2016b, The MathWorks, Inc., Natick, Massachusetts, United States) *robustfit* function including the factors group, age, and sex to calculate differences in FNC for each dynamic state separately. As in static FNC analyses, dynamic FNC analyses controlled for scanner site and motion parameters were regressed out. Again, we tested for effects on the individual ICN-to-ICN connections, as well as for effects on the domain averages. Results were corrected for multiple comparisons, applying FDR ($q = 0.05$).

Based on the dynamic states, summary metrics can be calculated describing the dynamic behavior for each participant across the resting state scan: (1) the mean dwell time (MDT) represents the time an individual spends in a certain state before switching to another state; (2) the fraction of time (FT) is the time an individual spends in one particular state relative to the entire scan time; and (3) the number of transitions (NT) represents how often one changes between different dynamic states. Again, the initial regression model included the factors group, age, and sex, prior to testing significant results for mediation effects of IQ and ADHD, as described above.

3.5. Meta-state analysis

One downside of the above-described dynamic FNC approach is that each windowed FNC matrix is assigned to the one state it shows highest correlation (similarity) with. This hard-clustering approach disregards some of the information contained in each FNC window. An approach to overcome this issue is meta-state analysis (Miller et al., 2016), in which, rather than assigning each FNC window to only one of the 3 dynamic states, a vector is created containing the distances from each FNC window to all of the dynamic states. This distance vector is then parametrized in such a way that each concrete value is replaced by $\pm$ {1,2,3,4} depending on the signed quartile, based on the distances of the entire group across the entire scan time. These meta-state vectors can then be used to calculate summary measures of higher-order brain dynamism that describe the dynamic fluidity and range of whole-brain

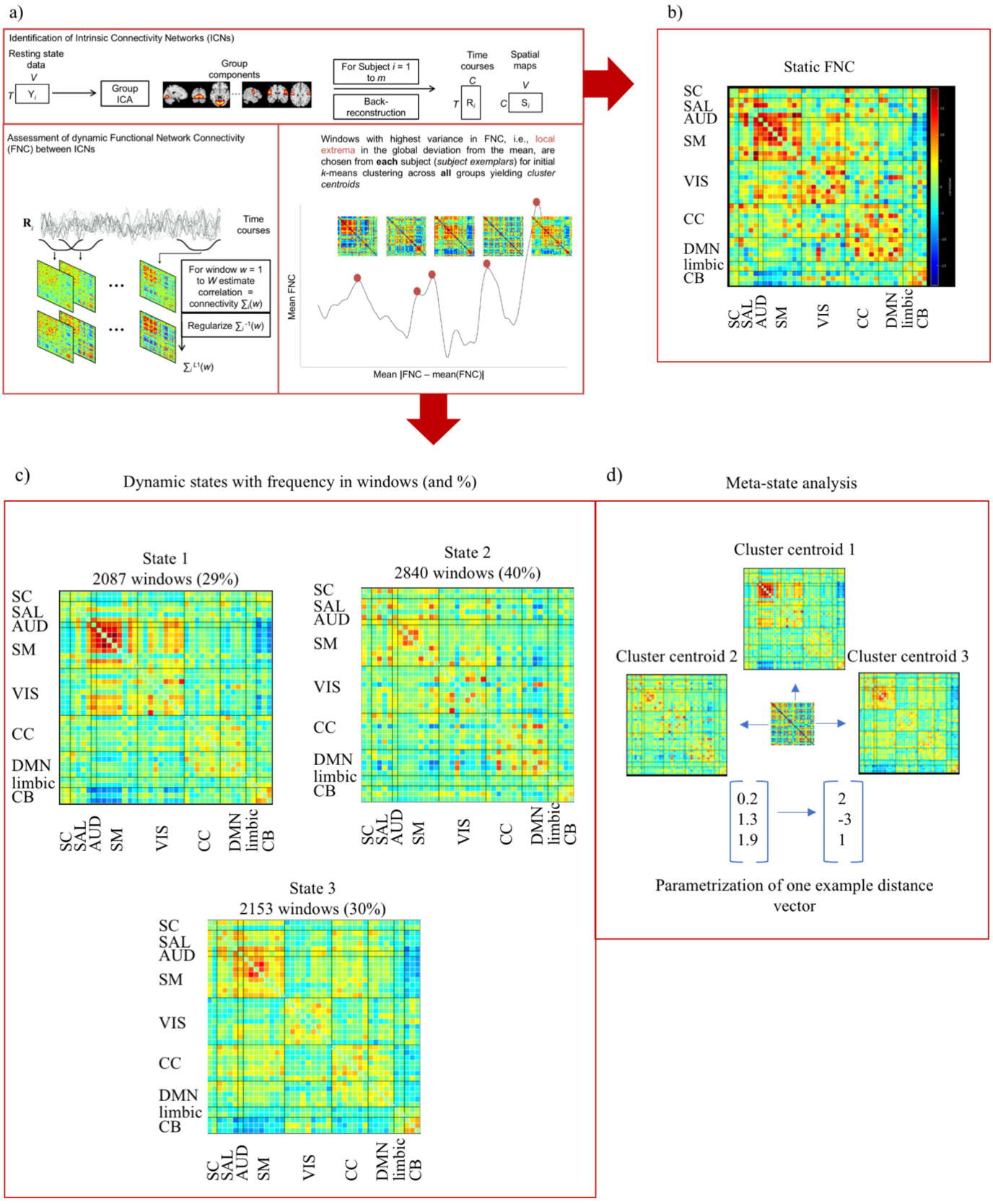

Fig. 1. a) Analysis steps of group ICA, b) static, and c) dynamic FNC across all participants, and d) construction of meta-state.
ICA – Independent Component Analysis, FNC – Functional Network Connectivity, SC – subcortical, SAL – salience, AUD – auditory, SM – sensorimotor, VIS – visual, CC – cognitive control domains, DMN – default mode network, CB – cerebellum.

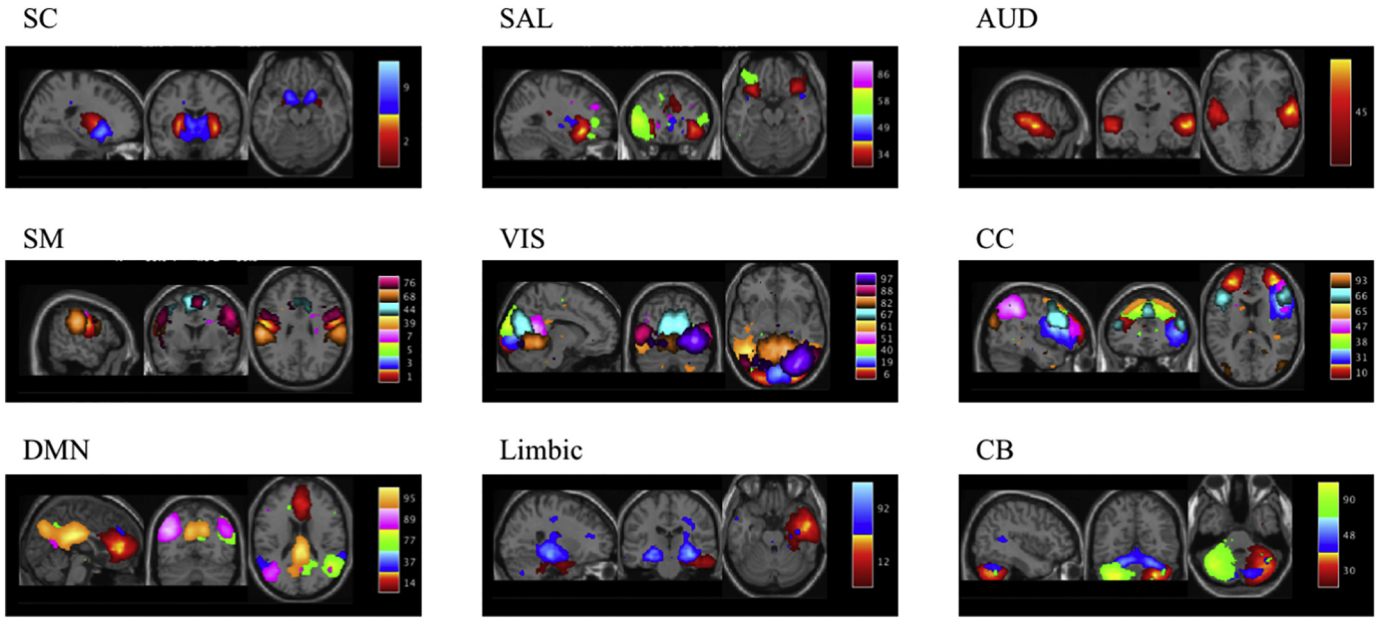

Fig. 2. Overview of the 41 Intrinsic Connectivity Networks, summarized in 9 functional domains.
SC – subcortical, SAL – salience, AUD – auditory, SM – sensorimotor, VIS – visual, CC – cognitive control, DMN – default mode network, CB – cerebellar domains.

connectivity. The number of unique meta-states and the number of changes of meta-states describe the dynamic fluidity of whole brain connectivity. The dynamic range is characterized by the longest L1 distance between two distinct meta-states (the span) and the total distance one subject "explores" in the *k*-dimensional meta-state space.

In order to test for group differences with regard to the four meta-state metrics (number of meta-states, meta-state changes, meta-state span, and the total distance), we applied regression analysis including the factors group, age, and sex. Then we tested any significant results for mediation effects of IQ and ADHD, as described above.

4. Results

4.1. Static FNC

Across groups, the static FNC matrix exhibits increased connectivity within each functional domain and anti-correlation between the cerebellum and the sensorimotor and auditory domains (Fig. 1b). Interestingly, the typically described anti-correlation between DMN and cognitive control domains is not observed (Fox et al., 2005).

Two ICN-to-ICN pairs exhibited significant differences between NF1 and HC participants. In particular, the middle frontal gyri (assigned to the cognitive control domain) showed hypoconnectivity with the cerebellum in NF1 relative to HC participants ($p < 0.0001$, mean connectivity HC = 0.23, mean connectivity NF1 = −0.01), whereas the cerebellum and the posterior middle temporal gyrus (multimodal association cortex (Binder et al., 2009; Visser et al., 2012)) exhibited less anticorrelation in NF1 participants ($p < 0.0001$, mean connectivity HC = −0.26, mean connectivity NF1 = −0.04). Further, intra-domain connectivity of the cognitive control domain was increased in NF1 individuals ($p = 0.0008$, mean connectivity HC = 0.12, mean connectivity NF1 = 0.2).

Post hoc mediation analysis of the above significant results showed a significant ADE of IQ only for the intra-domain connectivity in the cognitive control domain ($p = 0.02$, 95% confidence interval 0.018–0.15, point estimate 0.08): In other words, group has a significant effect on connectivity of the cognitive control domain even after correcting for covariates and potential mediation effects of IQ, in such a way that NF1 participants showed reduced connectivity within the cognitive control domain. However, there were no significant results for ADHD.

4.2. Dynamic FNC

Here, we identified 3 distinct dynamic states across groups, shown in Fig. 1c. In State 1 there is increased intra-domain connectivity of the sensorimotor domain relative to the other two states, and strong anti-correlated connectivity between the cerebellum and the sensorimotor domain. Overall, 29% of all FNC windows of all participants were assigned to this state. In state 2, connectivity within the cognitive control and DMN domains are slightly increased relative to the other two states, and parts of the DMN domain exhibit anti-correlation with ICNs of the salience, sensorimotor, and visual domains. Of all FNC windows, 40% were assigned to this state. State 3 is characterized by reduced connectivity within and between the functional domains, and anti-correlation is observed between the cerebellum and the salience, auditory, and sensorimotor domains. This somewhat hypoconnected state occurred in 30% of all FNC windows.

Interestingly, the DMN and cognitive control domains, typically described as showing antagonism (Fox et al., 2005), instead exhibited positive connectivity with each other, basically forming one coherent functional domain across all observed states. This observation is in accordance with recent studies showing that connectivity between the cognitive control domain and the DMN is variable, and not consistently anti-correlated (Dixon et al., 2017).

Main effects of group did not survive correction for multiple comparisons for any of the three dynamic states, nor were there significant main effects of age or sex.

4.3. Dynamic indices

With regard to the summary metrics describing each participant's dynamic behavior across the resting state scan, NF1 individuals showed significantly higher FT ($p = 0.019$) and MDT ($p = 0.02$) for state 3, the hypoconnected state. No significant group differences for FT and MDT of the other states were observed, and the number of transitions (NT) was also not significantly different between groups. Table 2 and Fig. 3 summarize MDT, FT, and NT across the three states. The mediation analysis of IQ and ADHD revealed no significant effects, indicating that neither IQ nor probable ADHD influence the time spent in particular

Table 2
Means (and standard deviations) for mean dwell times (MDT) in number of windows before a switch, mean fraction of time (FT; in percent) of the entire scan time, and number of total transitions (NT) for NF1 patients and Healthy Controls, across all states.

	MDT 1	MDT 2	MDT 3	FT 1	FT 2	FT 3	NT
HC	30.83 (29.42)	40.44 (35.24)	16.51* (23.46)	0.38 (0.32)	0.43 (0.32)	0.2* (0.28)	2.4 (1.9)
NF	18.82 (26.91)	35.98 (38.21)	36.72* (38.02)	0.21 (0.28)	0.38 (0.34)	0.41* (0.38)	1.9 (1.5)

* Significant group effect at $p < 0.05$.

dynamic states in this sample.

4.4. Meta-states

Even though NF1 participants exhibited lower values for all four meta-state summary metrics (number of meta-states, meta-state changes, meta-state span, and the total distance), the only significant difference was observed in the meta-state span: the longest distance between two distinct meta-states was significantly shorter in NF1 than in HC participants ($p = 0.023$), indicating a reduced range of whole-brain connectivity. Group means for all four measures are summarized in Table 3.

With regard to the IQ mediation analysis, the meta-state span exhibited a significant ADE for NF1 participants ($p = 0.03$, 95% CI -1.5 to -0.04, point estimate -0.8) indicating that group has a significant effect on meta-state span even after controlling for covariates and potential mediation effects of IQ. However, the ADHD mediation analysis revealed no significant effects.

5. Discussion

Only recently have studies begun to investigate the wealth of information contained within the temporal features of resting functional connectivity (Hutchison et al., 2013a). Here, we conducted the first investigation of static, dynamic, and higher-dimensional functional connectivity in one of the largest NF1 samples to date, applying new methods that have now been shown to be highly reproducible (Abrol et al., 2017).

Table 3
Means and standard deviations for meta-state summary measures: Number of meta-state changes, number of unique meta-states, longest distance between meta-states (state span), and total distance covered in the meta-state space.

	State changes	Number of states	State span	Total distance
HC	16.7 (4.6)	12.63 (4.21)	5.9* (0.99)	17.67 (4.71)
NF	14.67 (5.2)	10.6 (4.48)	5.0* (1.59)	15.63 (5.93)

* Significant group effect at $p < 0.05$.

5.1. Functional network connectivity

With regard to static resting connectivity, we found that connectivity of the cognitive control domain in particular appears compromised in NF1 patients. More precisely, connectivity between frontal brain areas within the cognitive control domain and the cerebellum is decreased in NF1. Even though the cerebellum is often neglected in functional MRI studies, recent evidence indicates that it is not only involved in motor tasks but indeed co-activates with brain areas involved in executive functioning (Stoodley et al., 2012; Stoodley and Schmahmann, 2010). Moreover, Reineberg et al. (2015) found that better performance in executive functioning tasks was associated with increased connectivity between the cerebellum and the frontopolar cortex. Here, however, we did not observe a significant mediation of fronto-cerebellar connectivity by IQ.

Interestingly though, a direct effect was identified for connectivity *within* the cognitive control domain, indicating that the intra-domain hyperconnectivity in NF1 participants was still present after controlling for covariates and possible mediating effects of IQ. Further, using a different graph theory analytic approach, Tomson et al. found similar

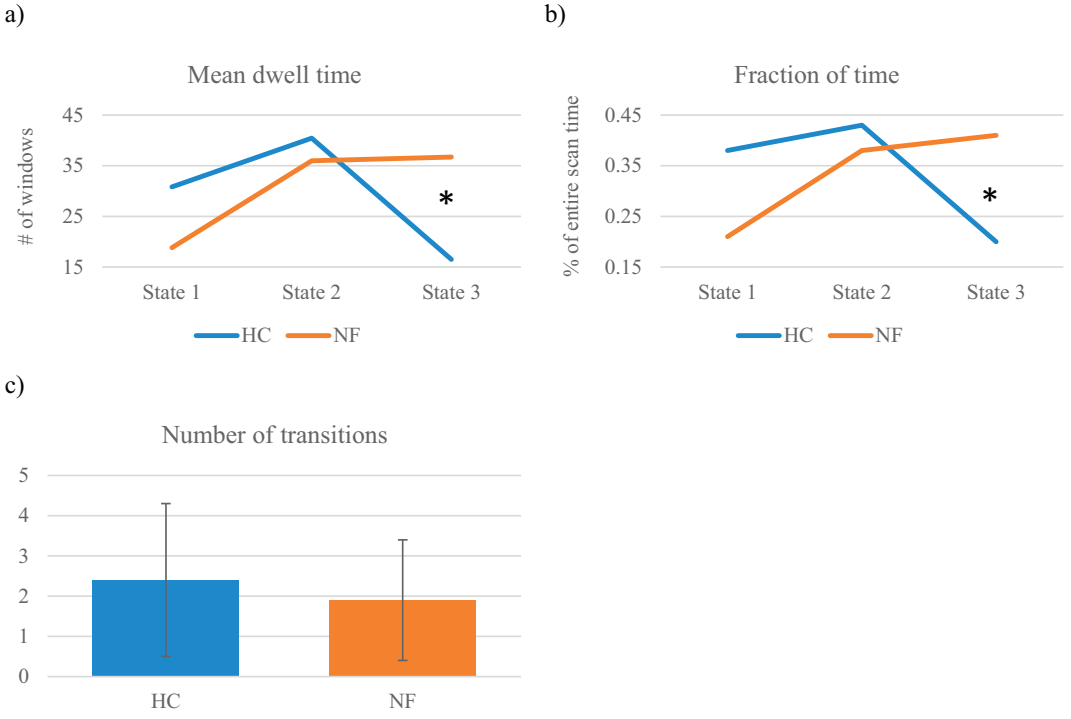

Fig. 3. Plots of a) the mean dwell time, b) fraction of time, and c) the number of transitions for NF1 patients (NF) and Healthy Controls (HC).
*Significant group effect at $p < 0.05$.

patterns of reduced anterior-to-posterior connectivity in the same sample of NF1 participants that were not related to IQ (Tomson et al., 2015). However, another small study found that increased connectivity between the frontal pole and ventral anterior cingulate cortex was correlated with cognitive and social deficits in NF1 patients (Loitfelder et al., 2015). Future, larger-scale studies and longitudinal studies are warranted to better understand the functional implications of altered functional connectivity in NF1.

The analysis of dynamic FNC did not indicate significant group differences and overall, static and dynamic FNC between distinct ICNs appears largely unimpaired in NF1 participants in the current study. However, it is important to bear in mind that even though this is one of the largest neuroimaging studies of NF1 to date, it is nevertheless underpowered to detect small to moderate effects. Furthermore, the relationships between morphological alterations and functional connectivity patterns in NF1 are not well understood; pathobiological factors such as disruptions of white matter microstructure and cortical neuroanatomic alterations (Duarte et al., 2014; Karlsgodt et al., 2012; Payne et al., 2010; Violante et al., 2013) might contribute to the lack of significance of dynamic FNC.

5.2. Dynamic indices and higher-dimensional dynamism

Despite the fact that ICN-to-ICN connectivity seems mostly intact in NF1 patients, summary measures and higher-order metrics of whole-brain connectivity dynamism indeed show alterations: specifically, NF1 patients spent more time in a hypoconnected dynamic state and had a reduced dynamic range of whole brain connectivity.

Similar results of a preference for hypoconnected states, as well as a reduction of the dynamic range of whole-brain connectivity, have been found in studies of patients with schizophrenia and individuals at clinical high risk for developing psychosis (Damaraju et al., 2014; Mennigen et al., in press; Miller et al., 2016). Interestingly, a recent study on youth with clinically-diagnosed ADHD found a distinct pattern of increased dwell time in a state of *heightened* connectivity within the DMN and *increased* meta-state span in ADHD youth relative to typically developing youth (de Lacy and Calhoun, 2018). Given the increased risk of ADHD in NF1 (Lidzba et al., 2012), one might anticipate findings of dynamic indices and higher-dimensional dynamism to be more similar to those in individuals with idiopathic ADHD. Thus, these contrasting findings highlight that both NF1 and ADHD are complex disorders, with differing patterns of time-varying connectivity that may result in similar downstream behavioral phenotypes.

Furthermore, since both dynamic FNC and meta-state analysis approaches have mostly been applied to individuals on the psychosis spectrum, the globally similar pattern of findings in NF1 and the psychosis spectrum might indicate a nonspecific impairment of connectivity dynamism across disorders that impact overall brain health. It is not yet known whether impairments relate to specific symptoms and/or executive functions across different disorders. A dimensional approach to investigate distinct psychopathologies may be informative in future studies.

5.3. Limitations

Certain limitations of this study must be noted. Even though the sample size is relatively large for this particular rare disorder, it is nevertheless small given current standards. Further, the current sample encompasses individuals from a wide age range of 10 to 46; although NF1 patients and controls were age-matched and age was included as a variable in all statistical models, developmental effects might interfere and/or overlap with disease-specific effects.

Here, we identified 3 dynamic states but in a recent study that examined replicability of dynamic FNC, the optimal number of clusters was estimated to be 5 across 28 groups with 250 individuals each (Abrol et al., 2017). However, the similarity of dynamic states in the current study was very high, independent on the number of clusters, and the lower k in the current sample may be due to the smaller sample size.

Furthermore, longer resting state scans and higher spatial resolution may allow for more stable estimations of dynamic FNC and this is a topic of ongoing research (Abrol et al., 2017; Hindriks et al., 2016; Preti et al., 2017).

6. Conclusion

Here, we present a comprehensive analysis of different aspects of functional network connectivity in NF1. In particular, NF1 individuals exhibit altered connectivity of the cognitive control domain relative to healthy control participants. Further, higher-dimensional dynamics of functional network connectivity are compromised in NF1 patients, which may reflect global brain dysfunction.

Acknowledgment

This study was funded by the National Institute of Mental Health (NIMH) R34 MH089299-01, the Department of Defense - Congressionally Directed Medical Research Program (DoD/CDMRP) W81XWH-12-1-0081, and National Institute of Health Roadmap grants UL1-DE019580 and PL1MH083271.

Appendix A. Supplementary data

Supplementary data to this article can be found online at https://doi.org/10.1016/j.nicl.2019.101692.

References

Abrol, A., Damaraju, E., Miller, R.L., Stephen, J.M., Claus, E.D., Mayer, A.R., Calhoun, V.D., 2017. Replicability of time-varying connectivity patterns in large resting state fMRI samples. NeuroImage 163, 160–176. https://doi.org/10.1016/j.neuroimage.2017.09.020.

Achenbach, 1991. Manual for the Child Behavior Checklist/ 4–18 and 1991 Profile. University of Vermont, Department of Psychiatry, Burlington, VT.

Adler, L.A., Spencer, T., Faraone, S.V., Kessler, R.C., Howes, M.J., Biederman, J., Secnik, K., 2006. Validity of Pilot Adult ADHD Self- Report Scale (ASRS) to Rate Adult ADHD Symptoms. Ann. Clin. Psychiatry 18, 145–148. https://doi.org/10.3109/10401230600801077.

Allen, E.A., Erhardt, E.B., Damaraju, E., Gruner, W., Segall, J.M., Silva, R.F., Havlicek, M., Rachakonda, S., Fries, J., Kalyanam, R., Michael, A.M., Caprihan, A., Turner, J.A., Eichele, T., Adelsheim, S., Bryan, A.D., Bustillo, J., Clark, V.P., Feldstein Ewing, S.W., Filbey, F., Ford, C.C., Hutchison, K., Jung, R.E., Kiehl, K.A., Kodituwakku, P., Komesu, Y.M., Mayer, A.R., Pearlson, G.D., Phillips, J.P., Sadek, J.R., Stevens, M., Teuscher, U., Thoma, R.J., Calhoun, V.D., 2011. A Baseline for the Multivariate Comparison of Resting-State Networks. Front. Syst. Neurosci. 5. https://doi.org/10.3389/fnsys.2011.00002.

Allen, E.A., Damaraju, E., Plis, S.M., Erhardt, E.B., Eichele, T., Calhoun, V.D., 2012a. Tracking Whole-Brain Connectivity Dynamics in the Resting State. Cereb. Cortex 24, 663–676. https://doi.org/10.1093/cercor/bhs352.

Allen, E.A., Erhardt, E.B., Wei, Y., Eichele, T., Calhoun, V.D., 2012b. Capturing inter-subject variability with group independent component analysis of fMRI data: a simulation study. NeuroImage 59, 4141–4159. https://doi.org/10.1016/j.neuroimage.2011.10.010.

Binder, J.R., Desai, R.H., Graves, W.W., Conant, L.L., 2009. Where is the Semantic System? A critical Review and Meta-Analysis of 120 Functional Neuroimaging Studies. Cereb. Cortex N. Y. NY 19, 2767–2796. https://doi.org/10.1093/cercor/bhp055.

Calhoun, V.D., Adali, T., 2012. Multisubject Independent Component Analysis of fMRI: a Decade of Intrinsic Networks, Default Mode, and Neurodiagnostic Discovery. IEEE Rev. Biomed. Eng. 5, 60–73. https://doi.org/10.1109/RBME.2012.2211076.

Calhoun, V.D., Adali, T., Pearlson, G.D., Pekar, J.j., 2001. A method for making group inferences from functional MRI data using independent component analysis. Hum. Brain Mapp. 14, 140–151. https://doi.org/10.1002/hbm.1048.

Chabernaud, C., Mennes, M., Kardel, P.G., Gaillard, W.D., Kalbfleisch, M.L., VanMeter, J.W., Packer, R.J., Milham, M.P., Castellanos, F.X., Acosta, M.T., 2012. Lovastatin regulates brain spontaneous low-frequency brain activity in Neurofibromatosis type 1. Neurosci. Lett. 515, 28–33. https://doi.org/10.1016/j.neulet.2012.03.009.

Chisholm, A.K., Anderson, V.A., Pride, N.A., Malarbi, S., North, K.N., Payne, J.M., 2018. Social Function and Autism Spectrum Disorder in Children and adults with Neurofibromatosis Type 1: a Systematic Review and Meta-Analysis. Neuropsychol. Rev. https://doi.org/10.1007/s11065-018-9380-x.

Costa, R.M., Federov, N.B., Kogan, J.H., Murphy, G.G., Stern, J., Ohno, M., Kucherlapati,

R., Jacks, T., Silva, A.J., 2002. Mechanism for the learning deficits in a mouse model of neurofibromatosis type 1. Nature 415, 526–530. https://doi.org/10.1038/nature711.

Damaraju, E., Allen, E.A., Belger, A., Ford, J.M., McEwen, S., Mathalon, D.H., Mueller, B.A., Pearlson, G.D., Potkin, S.G., Preda, A., Turner, J.A., Vaidya, J.G., van Erp, T.G., Calhoun, V.D., 2014. Dynamic functional connectivity analysis reveals transient states of dysconnectivity in schizophrenia. NeuroImage Clin. 5, 298–308. https://doi.org/10.1016/j.nicl.2014.07.003.

Damoiseaux, J.S., Greicius, M.D., 2009. Greater than the sum of its parts: a review of studies combining structural connectivity and resting-state functional connectivity. Brain Struct. Funct. 213, 525–533. https://doi.org/10.1007/s00429-009-0208-6.

de Lacy, N., Calhoun, V.D., 2018. Dynamic connectivity and the effects of maturation in youth with attention deficit hyperactivity disorder. Netw. Neurosci. 1–41. https://doi.org/10.1162/netn_a_00063.

Dixon, M.L., Andrews-Hanna, J.R., Spreng, R.N., Irving, Z.C., Mills, C., Girn, M., Christoff, K., 2017. Interactions between the default network and dorsal attention network vary across default subsystems, time, and cognitive states. NeuroImage 147, 632–649. https://doi.org/10.1016/j.neuroimage.2016.12.073.

Duarte, J.V., Ribeiro, M.J., Violante, I.R., Cunha, G., Silva, E., Castelo-Branco, M., 2014. Multivariate pattern analysis reveals subtle brain anomalies relevant to the cognitive phenotype in neurofibromatosis type 1. Hum. Brain Mapp. 35, 89–106. https://doi.org/10.1002/hbm.22161.

Erhardt, E.B., Rachakonda, S., Bedrick, E.J., Allen, E.A., Adali, T., Calhoun, V.D., 2011. Comparison of multi-subject ICA methods for analysis of fMRI data. Hum. Brain Mapp. 32, 2075–2095. https://doi.org/10.1002/hbm.21170.

First, M.B., Spitzer, R.L., Gibbon, M., Williams, J.B.W., 2002. Structured Clinical Interview for DSM-IV-TR Axis I Disorders, Research Version, Patient Edition. Biometrics Research, New York State Psychiatric Institute, New York.

Fox, M.D., Snyder, A.Z., Vincent, J.L., Corbetta, M., Essen, D.C.V., Raichle, M.E., 2005. The human brain is intrinsically organized into dynamic, anticorrelated functional networks. Proc. Natl. Acad. Sci. U. S. A. 102, 9673–9678. https://doi.org/10.1073/pnas.0504136102.

Garg, S., Green, J., Leadbitter, K., Emsley, R., Lehtonen, A., Evans, D.G., Huson, S.M., 2013. Neurofibromatosis Type 1 and Autism Spectrum Disorder. Pediatrics peds. 1868–2013. https://doi.org/10.1542/peds.2013-1868.

Gutmann, D.H., Wood, D.L., Collins, F.S., 1991. Identification of the neurofibromatosis type 1 gene product. Proc. Natl. Acad. Sci. 88, 9658–9662. https://doi.org/10.1073/pnas.88.21.9658.

Gutmann, D.H., Ferner, R.E., Listernick, R.H., Korf, B.R., Wolters, P.L., Johnson, K.J., 2017. Neurofibromatosis type 1. Nat. Rev. Dis. Primer 3, 17004. https://doi.org/10.1038/nrdp.2017.4.

Himberg, J., Hyvärinen, A., 2003. Icasso: Software for investigating the reliability of ICA estimates by clustering and visualization. In: Neural Networks for Signal Processing, 2003. NNSP'03. 2003 IEEE 13th Workshop On. IEEE, pp. 259–268.

Hindriks, R., Adhikari, M.H., Murayama, Y., Ganzetti, M., Mantini, D., Logothetis, N.K., Deco, G., 2016. Can sliding-window correlations reveal dynamic functional connectivity in resting-state fMRI? NeuroImage 127, 242–256. https://doi.org/10.1016/j.neuroimage.2015.11.055.

Honey, C.J., Sporns, O., Cammoun, L., Gigandet, X., Thiran, J.P., Meuli, R., Hagmann, P., 2009. Predicting human resting-state functional connectivity from structural connectivity. Proc. Natl. Acad. Sci. 106, 2035–2040. https://doi.org/10.1073/pnas.0811168106.

Hutchison, R.M., Womelsdorf, T., Allen, E.A., Bandettini, P.A., Calhoun, V.D., Corbetta, M., Della Penna, S., Duyn, J.H., Glover, G.H., Gonzalez-Castillo, J., Handwerker, D.A., Keilholz, S., Kiviniemi, V., Leopold, D.A., de Pasquale, F., Sporns, O., Walter, M., Chang, C., 2013a. Dynamic functional connectivity: promise, issues, and interpretations. NeuroImage 80, 360–378. https://doi.org/10.1016/j.neuroimage.2013.05.079. Mapping the Connectome.

Hutchison, R.M., Womelsdorf, T., Gati, J.S., Everling, S., Menon, R.S., 2013b. Resting-state networks show dynamic functional connectivity in awake humans and anesthetized macaques. Hum. Brain Mapp. 34, 2154–2177. https://doi.org/10.1002/hbm.22058

Hyman, S.L., Shores, A., North, K.N., 2005. The nature and frequency of CME cognitive deficits in children with neurofibromatosis type. Neurology 65, 1037–1044.

Imai, K., Keele, L., Tingley, D., 2010a. A general approach to causal mediation analysis. Psychol. Methods 15, 309–334. https://doi.org/10.1037/a0020761.

Imai, K., Keele, L., Yamamoto, T., 2010b. Identification, inference and sensitivity analysis for causal mediation effects. Stat. Sci. 25, 51–71.

Imai, K., Keele, L., Tingley, D., Yamamoto, T., 2011. Unpacking the Black Box of Causality: Learning about Causal Mechanisms from Experimental and Observational Studies. Am. Polit. Sci. Rev. 105, 765–789. https://doi.org/10.1017/S0003055411000414.

Jenkinson, M., Bannister, P., Brady, M., Smith, S., 2002. Improved optimization for the robust and accurate linear registration and motion correction of brain images. NeuroImage 17, 825–841. https://doi.org/10.1006/nimg.2002.1132.

Karlsgodt, K.H., Rosser, T., Lutkenhoff, E.S., Cannon, T.D., Silva, A., Bearden, C.E., 2012. Alterations in White Matter Microstructure in Neurofibromatosis-1. PLoS One 7, e47854. https://doi.org/10.1371/journal.pone.0047854.

Kessler, R.C., Adler, L., Ames, M., Demler, O., Faraone, S., Hiripi, E., Howes, M.J., Jin, R., Secnik, K., Spencer, T., Ustun, T.B., Walters, E.E., 2005. The World Health Organization adult ADHD self-report scale (ASRS): a short screening scale for use in the general population. Psychol. Med. 35, 245–256. https://doi.org/10.1017/S0033291704002892.

Kessler, R.C., Adler, L.A., Gruber, M.J., Sarawate, C.A., Spencer, T., Brunt, D.L.V., 2007. Validity of the World Health Organization Adult ADHD Self-Report Scale (ASRS) Screener in a representative sample of health plan members. Int. J. Methods Psychiatr. Res. 16, 52–65. https://doi.org/10.1002/mpr.208.

Lidzba, K., Granström, S., Lindenau, J., Mautner, V.-F., 2012. The adverse influence of attention-deficit disorder with or without hyperactivity on cognition in neurofibromatosis type 1. Dev. Med. Child Neurol. 54, 892–897. https://doi.org/10.1111/j.1469-8749.2012.04377.x.

Loitfelder, M., Huijbregts, S.C.J., Veer, I.M., Swaab, H.S., Van Buchem, M.A., Schmidt, R., Rombouts, S.A., 2015. Functional connectivity changes and executive and social problems in neurofibromatosis Type I. Brain Connect. 5, 312–320. https://doi.org/10.1089/brain.2014.0334.

Luna, B., Marek, S., Larsen, B., Tervo-Clemmens, B., Chahal, R., 2015. An integrative model of the maturation of cognitive control. Annu. Rev. Neurosci. 38, 151–170. https://doi.org/10.1146/annurev-neuro-071714-034054.

Matsui, T., Murakami, T., Ohki, K., 2018. Neuronal origin of the temporal dynamics of spontaneous BOLD activity correlation. Cereb. Cortex. https://doi.org/10.1093/cercor/bhy045.

Mennigen, E., Miller, R.L., Rashid, B., Fryer, S.L., Loewy, R.L., Stuart, B.K., Mathalon, D.H., Calhoun, V.D., (in press). Reduced higher-dimensional resting state fMRI dynamism in clinical high-risk individuals for schizophrenia identified by meta-state analysis. Schizophr. Res. https://doi.org/10.1016/j.schres.2018.06.007

Miller, R.L., Yaesoubi, M., Turner, J.A., Mathalon, D.H., Preda, A., Pearlson, G., Adali, T., Calhoun, V.D., 2016. Higher Dimensional Meta-State Analysis reveals Reduced Resting fMRI Connectivity Dynamism in Schizophrenia patients. PLoS One 11, e0149849. https://doi.org/10.1371/journal.pone.0149849.

Payne, J.M., Moharir, M.D., Webster, R., North, K.N., 2010. Brain structure and function in neurofibromatosis type 1: current concepts and future directions. J. Neurol. Neurosurg. Psychiatry 81, 304–309. https://doi.org/10.1136/jnnp.2009.179630.

Poldrack, R.A., Congdon, E., Triplett, W., Gorgolewski, K.J., Karlsgodt, K.H., Mumford, J.A., Sabb, F.W., Freimer, N.B., London, E.D., Cannon, T.D., Bilder, R.M., 2016. A phenome-wide examination of neural and cognitive function. Sci. Data 3, 160110. https://doi.org/10.1038/sdata.2016.110.

Power, J.D., Mitra, A., Laumann, T.O., Snyder, A.Z., Schlaggar, B.L., Petersen, S.E., 2014. Methods to detect, characterize, and remove motion artifact in resting state fMRI. NeuroImage 84, 320–341. https://doi.org/10.1016/j.neuroimage.2013.08.048.

Preti, M.G., Bolton, T.A., Van De Ville, D., 2017. The dynamic functional connectome: State-of-the-art and perspectives. NeuroImage, Funct. Archit. Brain 160, 41–54. https://doi.org/10.1016/j.neuroimage.2016.12.061.

Reineberg, A.E., Andrews-Hanna, J.R., Depue, B.E., Friedman, N.P., Banich, M.T., 2015. Resting-state networks predict individual differences in common and specific aspects of executive function. NeuroImage 104, 69–78. https://doi.org/10.1016/j.neuroimage.2014.09.045.

Roessner, V., Becker, A., Rothenberger, A., Rohde, L.A., Banaschewski, T., 2007. A cross-cultural comparison between samples of Brazilian and German children with ADHD/HD using the Child Behavior Checklist. Eur. Arch. Psychiatry Clin. Neurosci. 257, 352–359. https://doi.org/10.1007/s00406-007-0738-y.

Roweis, S., 1998. EM algorithms for PCA and SPCA. Adv. Neural Inf. Proces. Syst. 626–632.

Skudlarski, P., Jagannathan, K., Calhoun, V.D., Hampson, M., Skudlarska, B.A., Pearlson, G., 2008. Measuring Brain Connectivity: Diffusion Tensor Imaging Validates Resting State Temporal Correlations. NeuroImage 43, 554–561. https://doi.org/10.1016/j.neuroimage.2008.07.063.

Stoodley, C.J., Schmahmann, J.D., 2010. Evidence for topographic organization in the cerebellum of motor control versus cognitive and affective processing. Cortex 46, 831–844. https://doi.org/10.1016/j.cortex.2009.11.008.

Stoodley, C.J., Valera, E.M., Schmahmann, J.D., 2012. Functional topography of the cerebellum for motor and cognitive tasks: an fMRI study. NeuroImage 59, 1560–1570. https://doi.org/10.1016/j.neuroimage.2011.08.065.

Tomson, S.N., Schreiner, M.J., Narayan, M., Rosser, T., Enrique, N., Silva, A.J., Allen, G.I., Bookheimer, S.Y., Bearden, C.E., 2015. Resting state functional MRI reveals abnormal network connectivity in neurofibromatosis 1. Hum. Brain Mapp. 36, 4566–4581. https://doi.org/10.1002/hbm.22937.

Tzourio-Mazoyer, N., Landeau, B., Papathanassiou, D., Crivello, F., Etard, O., Delcroix, N., Mazoyer, B., Joliot, M., 2002. Automated Anatomical labeling of Activations in SPM using a Macroscopic Anatomical Parcellation of the MNI MRI Single-Subject Brain. NeuroImage 15, 273–289. https://doi.org/10.1006/nimg.2001.0978.

van den Heuvel, M.P., Mandl, R.C.W., Kahn, R.S., Pol, H.E.H., 2009. Functionally linked resting-state networks reflect the underlying structural connectivity architecture of the human brain. Hum. Brain Mapp. 30, 3127–3141. https://doi.org/10.1002/hbm.20737.

Violante, I.R., Ribeiro, M.J., Silva, E.D., Castelo-Branco, M., 2013. Gyrification, cortical and subcortical morphometry in neurofibromatosis type 1: an uneven profile of developmental abnormalities. J. Neurodev. Disord. 5, 3. https://doi.org/10.1186/1866-1955-5-3.

Visser, M., Jefferies, E., Embleton, K.V., Lambon Ralph, M.A., 2012. Both the Middle Temporal Gyrus and the Ventral Anterior Temporal Area are crucial for Multimodal Semantic Processing: Distortion-corrected fMRI evidence for a double Gradient of Information Convergence in the Temporal Lobes. J. Cogn. Neurosci. 24, 1766–1778. https://doi.org/10.1162/jocn_a_00244.

Wechsler, 1999. Wechsler abbreviated scale of intelligence. In: The Psychological Corporation. TX, San Antonio.